

200–400 μ l 4% paraformaldehyde (PFA) (number S898-07 JT Baker). Approximately 2×10^6 cells were evaluated for forward and side scatter characteristics by flow cytometry under the direction of J. Nordberg at the VA Core Flow Facility to determine the relative percentage of lymphocytes, monocytes and granulocytes. For oxidative burst assay, blood was collected and lysed as above then resuspended at 4 °C in approximately 200 μ l endotoxin and pyrogen-free PBS without Ca^{2+} and Mg^{2+} (number 70013-032, Gibco BRL) containing 5 mM glucose (Sigma number G5146). Before the oxidative burst assay, 200 μ l of PBS at 37 °C containing 1.5 mM Mg^{2+} and 1.0 mM Ca^{2+} was added to the cell suspension. The Fc OxyBURST Green Assay Reagent (Molecular probes number F-2902) was used to evaluate cell uptake and oxidative burst activity. Background fluorescence was recorded, then oxidative burst reagent added to a concentration of 30 μ g ml⁻¹ (5 μ l).

Whole blood killing assay

Fresh mouse blood was collected as above and 35 μ l added to 10 μ l of THB containing (1–2) $\times 10^6$ c.f.u of freshly diluted log-phase GAS. The mixture was incubated for 1 h at 37 °C with gentle agitation, and dilutions of the mixture plated on agar plates for enumeration of c.f.u. The growth index was calculated as the ratio of bacterial c.f.u. recovered versus the initial bacterial inoculum. Student's *t*-test analysis was performed using the Microsoft Excel statistical package.

Received 28 June; accepted 1 October 2001.

1. Scott, M. G. & Hancock, R. E. Cationic antimicrobial peptides and their multifunctional role in the immune system. *Crit. Rev. Immunol.* **20**, 407–431 (2000).
2. Boman, H. G. Innate immunity and the normal microflora. *Immunol. Rev.* **173**, 5–16 (2000).
3. Ganz, T. & Lehrer, R. Antibiotic peptides from higher eukaryotes: biology and applications. *Mol. Med. Today* **5**, 292–297 (1999).
4. Ganz, T. *et al.* Defensins: natural peptide antibiotics of human neutrophils. *J. Clin. Invest.* **76**, 1427–1435 (1985).
5. Zasloff, M. Magainins, a class of antimicrobial peptides from *Xenopus* skin: Isolation, characterization of two active forms, and partial cDNA sequence of a precursor. *Proc. Natl Acad. Sci. USA* **84**, 5449–5453 (1987).
6. Goldman, M. J. *et al.* Human β -defensin-1 is a salt-sensitive antibiotic in lung that is inactivated in cystic fibrosis. *Cell* **88**, 553–560 (1997).
7. Wang, Y., Agerberth, B., Lohgren, A., Almstedt, A. & Johansson, J. Apolipoprotein A-1 binds and inhibits the human antibacterial/cytotoxic peptide LL-37. *J. Biol. Chem.* **273**, 33115–33118 (1998).
8. Travis, S. M. *et al.* Bactericidal activity of mammalian cathelicidin-derived peptides. *Infect. Immun.* **68**, 2748–2755 (2000).
9. Gallo, R. L. *et al.* Syndecans, cell surface heparan sulfate proteoglycans, are induced by a proline-rich antimicrobial peptide from wounds. *Proc. Natl Acad. Sci. USA* **91**, 11035–11039 (1994).
10. Shi, J., Ross, C., Leto, T. & Blecha, F. PR-39, a proline-rich antibacterial peptide that inhibits phagocyte NADPH oxidase activity by binding to Src homology 3 domains of p47^{phox}. *Proc. Natl Acad. Sci. USA* **93**, 6014–6018 (1996).
11. Lencer, W. *et al.* Induction of epithelial chloride secretion by channel-forming cryptidins 2 and 3. *Proc. Natl Acad. Sci. USA* **94**, 8585–8589 (1997).
12. Rizzo, A., Zanetti, M. & Gennaro, R. Cytotoxicity and apoptosis mediated by two peptides of innate immunity. *Cell. Immunol.* **189**, 107–115 (1998).
13. Chertov, O. *et al.* Identification of defensin-1, defensin-2, and CAP37/azurocidin as T-cell chemoattractant proteins released from interleukin-8-stimulated neutrophils. *J. Biol. Chem.* **271**, 2935–2940 (1996).
14. Zanetti, M., Gennaro, R., Scocchi, M. & Skerlavaj, B. Structure and biology of cathelicidins. *Adv. Exp. Med. Biol.* **479**, 203–218 (2000).
15. Gudmundsson, G. H. *et al.* The human gene *Fall39* and processing of the cathelin precursor to the antibacterial peptide LL-37 in granulocytes. *Eur. J. Biochem.* **238**, 325–332 (1996).
16. Gallo, R. L. *et al.* Identification of CRAMP, a cathelin-related antimicrobial peptide expressed in the embryonic and adult mouse. *J. Biol. Chem.* **272**, 13088–13093 (1997).
17. Dorschner, R. A. *et al.* Cutaneous injury induces the release of cathelicidin antimicrobial peptides active against group A *Streptococcus*. *J. Invest. Dermatol.* **117**, 91–97 (2001).
18. Ferretti, J. J. *et al.* Complete genome sequence of an M1 strain of *Streptococcus pyogenes*. *Proc. Natl Acad. Sci. USA* **98**, 4658–4663 (2001).
19. Peekhaus, N. & Conway, T. Positive and negative transcriptional regulation of the *Escherichia coli* gluconate regulon gene *gntT* by GntR and the cyclic AMP (cAMP)–cAMP receptor protein complex. *J. Bacteriol.* **180**, 1777–1785 (1998).
20. Miller, S. I., Pulkkinen, W. S., Selsted, M. M. & Mekalanos, J. J. Characterization of defensin resistance phenotypes associated with mutations in the *phoP* virulence regulon of *Salmonella typhimurium*. *Infect. Immun.* **58**, 3706–3710 (1990).
21. Burtnick, M. N. & Woods, D. E. Isolation of polymyxin B-susceptible mutants of *Burkholderia pseudomallei* and molecular characterization of genetic loci involved in polymyxin B resistance. *Antimicrob. Agents Chemother.* **43**, 2648–2656 (1999).
22. Cole, A. M. *et al.* Inhibition of neutrophil elastase prevents cathelicidin activation and impairs clearance of bacteria from wounds. *Blood* **97**, 297–304 (2001).
23. Groisman, E. A., Parra-Lopez, C., Salcedo, M., Lippes, C. J. & Heffron, F. Resistance to host antimicrobial peptides is necessary for *Salmonella* virulence. *Proc. Natl Acad. Sci. USA* **89**, 11939–11943 (1992).
24. Islam, D. *et al.* Downregulation of bactericidal peptides in enteric infections: A novel immune escape mechanism with bacterial DNA as a potential regulator. *Nature Med.* **7**, 180–185 (2001).
25. Bals, R., Weiner, D., Meegalla, R. & Wilson, J. Transfer of a cathelicidin peptide antibiotic gene restores bacterial killing in a cystic fibrosis xenograft model. *J. Clin. Invest.* **103**, 1113–1117 (1999).
26. De, Y. *et al.* LL-37, the neutrophil granule- and epithelial cell-derived cathelicidin, utilizes formyl peptide receptor-like 1 (FPR1) as a receptor to chemoattract human peripheral blood neutrophils, monocytes, and T cells. *J. Exp. Med.* **192**, 1069–1074 (2000).
27. Yang, D. *et al.* β -defensins: linking innate and adaptive immunity through dendritic and T cell CCR6. *Science* **286**, 525–528 (1999).
28. Nizet, V. *et al.* Genetic locus for streptolysin S production by group A streptococcus. *Infect. Immun.* **68**, 4245–4254 (2000).

29. Karlyshev, A. V., Pallen, M. J. & Wren, B. W. Single-primer PCR procedure for rapid identification of transposon insertion sites. *Biotechniques* **28**, 1078–1082 (2000).
30. Betschel, S., Borgia, S., Barg, N., Low, D. & De Azavedo, J. Reduced virulence of group A streptococcal Tn916 mutants that do not produce streptolysin S. *Infect. Immun.* **66**, 1671–1679 (1998).

Acknowledgements

This work was supported by grants from the NIH (R.L.G. and V.N.), a VA merit award (R.L.G.), and grants from the American Skin Association (R.L.G.) and the Rockefeller Brothers Foundation (V.N.).

Correspondence and requests for materials should be addressed to R.L.G. (e-mail: rgallo@vapop.ucsd.edu).

.....
The E2F1–3 transcription factors are essential for cellular proliferation

Lizhao Wu*, **Cynthia Timmers***, **Baidehi Maiti***, **Harold I. Saavedra***, **Ling Sang***, **Gabriel T. Chong***, **Faison Nuckolls†**, **Paloma Giangrande†**, **Fred A. Wright***, **Seth J. Field‡**, **Michael E. Greenberg‡**, **Stuart Orkin§**, **Joseph R. Nevins†**, **Michael L. Robinson||** & **Gustavo Leone***

* *Division of Human Cancer Genetics, Department of Molecular Virology, Immunology and Medical Genetics, and Department of Molecular Genetics; and || Division of Molecular and Human Genetics, Children's Research Institute, The Ohio State University, Columbus, Ohio 43210, USA*
 † *Department of Genetics, Howard Hughes Medical Institute, Duke University Medical Center, Durham, North Carolina 27710, USA*
 ‡ *Department of Neuroscience, § Howard Hughes Medical Institute, Children's Hospital, Harvard Medical School, Boston, Massachusetts 02115, USA*

.....
The retinoblastoma tumour suppressor (Rb) pathway is believed to have a critical role in the control of cellular proliferation by regulating E2F activities^{1,2}. E2F1, E2F2 and E2F3 belong to a subclass of E2F factors thought to act as transcriptional activators important for progression through the G1/S transition³. Here we show, by taking a conditional gene targeting approach, that the combined loss of these three E2F factors severely affects E2F target expression and completely abolishes the ability of mouse embryonic fibroblasts to enter S phase, progress through mitosis and proliferate. Loss of E2F function results in an elevation of p21^{Cip1} protein, leading to a decrease in cyclin-dependent kinase activity and Rb phosphorylation. These findings suggest a function for this subclass of E2F transcriptional activators in a positive feedback loop, through down-modulation of p21^{Cip1}, that leads to the inactivation of Rb-dependent repression and S phase entry. By targeting the entire subclass of E2F transcriptional activators we provide direct genetic evidence for their essential role in cell cycle progression, proliferation and development.

The delineation of a pathway controlling the progression of cells out of quiescence, through G1 and into S phase, has been established^{1,2}. Principal events in this pathway include the activation of cyclin-dependent kinases (CDKs), the coordinated phosphorylation of Rb and p130 by cyclin–CDK complexes, and the subsequent release and accumulation of E2F activities^{1,2}. Although E2F has an essential role in control of cell growth during *Drosophila* development^{4,5}, current knockout mouse models have failed to demonstrate a similar requirement for any E2F family member in mammals^{6–12}. One interpretation of these observations is that under normal circumstances, loss of a single E2F member can be functionally compensated by other related E2F activities.

Of the six known E2F family members, E2F1, E2F2 and E2F3 can specifically interact with Rb, and their expression is cell-cycle regulated^{13,14}. To test for functional redundancy among this subclass

E2F1 and E2F2 cooperate with E2F3 to sustain normal proliferation and suggest that the severe growth defect resulting from their loss leads to the early embryonic lethality of $E2F1^{-/-}E2F3^{-/-}$ or $E2F2^{-/-}E2F3^{-/-}$ animals.

To confirm that loss of E2F3 was the primary factor responsible for the lack of growth observed on Cre treatment of $E2F1^{-/-}E2F2^{-/-}E2F3^{fl/fl}$ cells, we assessed the ability of Myc-tagged versions of $E2F3a$ and $E2F3b$ to rescue the growth defect of triple-knockout (TKO) cells. Western blot analysis demonstrated that the levels of ectopically expressed E2F3 proteins were similar to those of endogenous E2F3 normally found in wild-type or $E2F3$ -floxed cells (Fig. 2c). Reintroduction of E2F3a or E2F3b partially restored the colony-forming ability of TKO cells, and the combined expression of both proteins almost completely rescued the defect in colony formation (Fig. 2d). Furthermore, PCR genotyping confirmed that in cells where E2F3a and/or E2F3b was reintroduced, most of the emerging colonies were deleted for exon 3 (Fig. 2e), demonstrating that the rescue was due to the ectopic expression of E2F3 proteins and not to a failure in the Cre-mediated ablation of E2F3.

The proliferation assays described above suggest a particularly important function for E2F3 in growth control, but also show significant contributions made by E2F1 and E2F2 towards the control of cellular proliferation. These data, however, can not

distinguish between a model where individual E2F transcription factors might execute specific functions, such as the regulation of unique sets of gene targets, or a model where each E2F would contribute towards a pool of total E2F activity. To address this issue we sought to rescue the growth phenotype of TKO cells with haemagglutinin (HA)-tagged versions of each E2F activator. The results shown in Supplementary Information Fig. 2 indicate that E2F2 could only partially rescue the growth defect of TKO cells. Western blot assays indicated that E2F2 and E2F3 were expressed to equivalent levels, but E2F1 was consistently expressed at lower levels (Supplementary Information Fig. 2). The inherent ability of E2F1 to induce apoptosis probably led to the selection of cells with low expression of E2F1, making the comparison of their growth properties with those cells expressing exogenous E2F2 or E2F3 difficult to evaluate. Although some redundancy in their function is evident, our current data support a model where each E2F activator contributes unique functions towards the control of cell cycle and proliferation. The replacement of specific E2Fs by other family members using knock-in strategies *in vivo* might provide more definitive answers to this issue of functional specificity among E2F family members.

We next addressed whether the reduced growth rates of E2F mutant MEFs could be attributed to a specific defect in the G1/S transition. MEFs treated with either the Cre-expressing or control virus were synchronized by serum deprivation, then stimulated to proliferate by the addition of serum, and assayed for E2F-target gene activation and S-phase entry. Although peak levels of E2F target genes were not markedly affected by loss of E2F3 alone, their normal serum-induced accumulation was delayed by 2–3 h, a delay that was augmented further by the additional loss of either E2F1 or E2F2 (Supplementary Information Fig. 3 and data not shown). Cells deficient for all three E2F activators failed to induce many, but not all, E2F target genes in response to serum, including *Dhfr*, *Cdc6*, *Mcm3*, thymidine kinase (*Tk*) and DNA polymerase α (*DNA pol\alpha*) (Fig. 3). Moreover, the low levels of these transcripts in unsynchronized cell populations correlated with their inability to be induced by serum (Fig. 3a, both lanes labelled P). Notably, other putative E2F targets, including the *cyclin E* gene, were consistently elevated in quiescent TKO cells, were further induced on serum stimulation, and their levels remained relatively unaffected in unsynchronized cell populations (Fig. 3a, top panel). This finding is consistent with these targets being regulated mainly by Rb-mediated repression. Finally, reintroduction of E2F3 into TKO cells restored the normal activation of E2F target genes that occurs after mitogenic induction of quiescent cells (Fig. 3b). The levels of exogenous E2F3 protein introduced into these cells were nearly physiological, as indicated by western blot assays and its inability to activate E2F targets under conditions of low serum (Figs 2c and 3b, time 0). These findings support the idea that E2F activators are critical factors important for cell-cycle-dependent gene expression.

Cre-mediated loss of E2F3 from each of the E2F3-floxed cell lines impaired S phase entry, as measured by incorporation of 5-bromodeoxyuridine (BrdU) (Fig. 4a), to an extent that correlated with the severity of the proliferation and target activation defects described above. The defect of cell cycle entry of TKO cells is not due to their general inability to respond to growth signals, as the growth-factor-induced activation of the mitogen-activated protein kinase and phosphatidylinositol-3-OH kinase immediate-early pathways remained unaffected by the loss of E2F family members (Supplementary Information Fig. 3c). These findings indicate that E2F members grouped in the activator subclass, namely E2F1, E2F2 and E2F3, function at the G1/S transition to regulate entry into S phase and thereby promote cellular proliferation.

To determine whether the loss of E2F function would lead to an accumulation of cells in a specific phase of the cell cycle, TKO cells were analysed for DNA content by flow cytometry. As shown in Fig. 4b, control virus-treated $E2F1^{-/-}E2F2^{-/-}E2F3^{fl/fl}$ cells, rendered

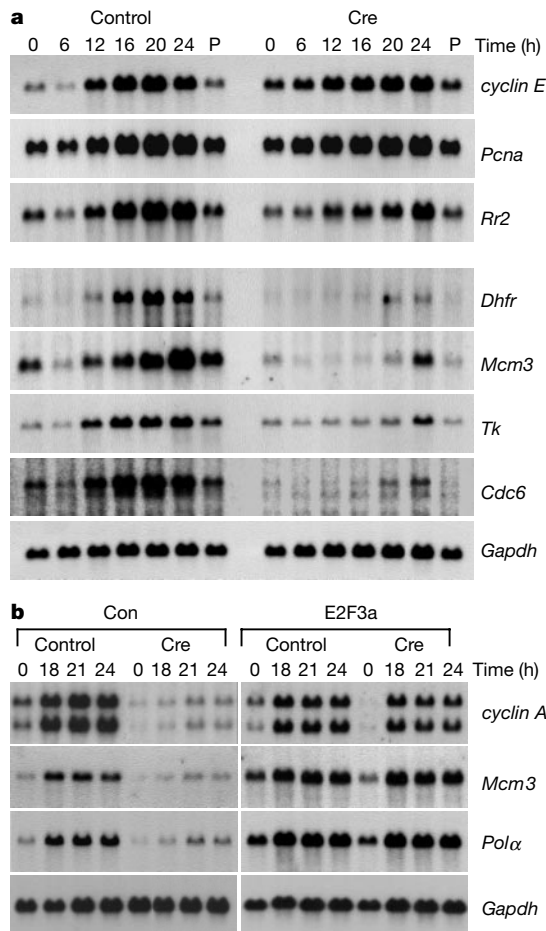


Figure 3 E2F activators regulate G1/S-specific target gene activation. **a**, Northern blot analysis of various E2F-responsive genes in $E2F1^{-/-}E2F2^{-/-}E2F3^{fl/fl}$ MEFs that were infected with a control or a Cre retrovirus. Serum-starved MEFs were induced to re-enter the cell cycle by addition of serum. RNA was extracted from serum-starved cells and serum-stimulated cells at different time points. P, proliferating cells. **b**, Northern blot analysis of various E2F-responsive genes in $E2F1^{-/-}E2F2^{-/-}E2F3^{fl/fl}$ MEFs that were treated in **a**. Con, pBhygro; E2F3a, pBhygro-myc-tagged E2F3a. *Gapdh* was used as a probe to verify equal loading.

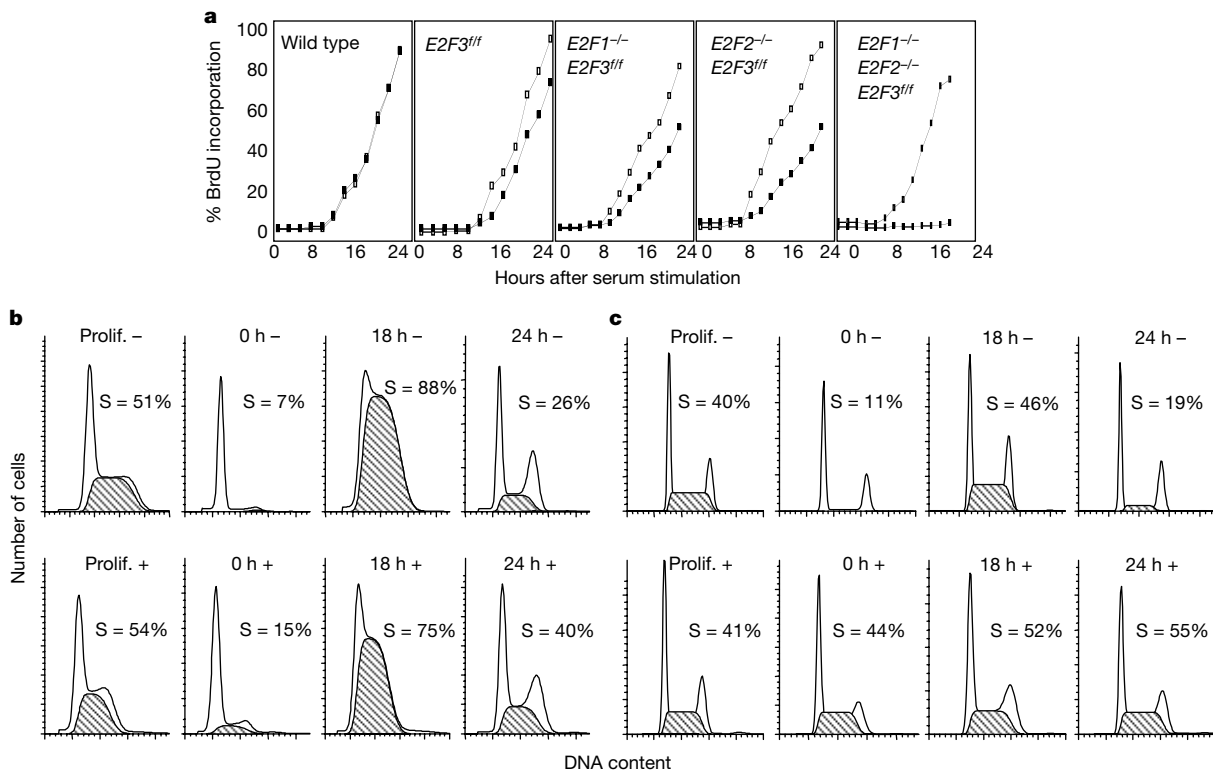


Figure 4 E2Fs are required for S phase entry and cell cycle progression. **a**, BrdU incorporation assays of MEFs that were infected with a control (open boxes) or a Cre retrovirus. **b, c**, Cell cycle analysis by FACS for wild-type MEFs (**c**) or *E2F1^{-/-}E2F2^{-/-}E2F3^{fl/fl}* MEFs (**c**) that were infected with a control (top panels (-)) or a Cre retrovirus (bottom

panels (+)). In **c**, a fraction of cells had become tetraploid by the time the experiment was performed, as indicated by the appearance of two distinct peaks in serum-starved samples (0 h). Hatched areas indicate the percentage of cells (S) containing an S-phase content of DNA.

quiescent by serum deprivation, accumulated a G1 content of DNA, and could be efficiently induced to enter the cell cycle after serum addition, as suggested by the timely accumulation of an S phase content of DNA. The similar profiles of control- and Cre-treated wild-type cells indicated that expression of Cre itself had little or no effect on the ability of cells to proliferate or progress through the cell cycle (Fig. 4b). Unsynchronized TKO cell populations had a similar profile of DNA content as control cells, except that most of these cells were also negative for BrdU incorporation (Fig. 4c, compare top and bottom samples; and data not shown). Moreover, TKO cells failed to accumulate a G1 content of DNA on serum deprivation and failed to respond to serum addition (Fig. 4c). Together, these findings show that ablation of all three E2F family members arrests cell growth irrespective of cell cycle position, indicating a role for these E2Fs throughout the cell cycle. Recent work also suggests a continuing role for E2F during S phase that seems to be important for the regulation of mitotic regulators and progression of cells through G2/M¹⁶. This view is consistent with recent genome-wide analyses of cell-cycle-regulated genes, where a large fraction of E2F-regulated gene targets were found to encode proteins known to be involved in the progression of cells into G2 and through mitosis^{17,18}.

To identify relevant downstream activities that might be responsible for mediating the growth arrest observed upon loss of E2F3, we assessed the status of various inhibitors of the cell cycle. Whereas p53 or p27^{Kip1} remained unchanged, p21^{Cip1} protein levels were markedly elevated in TKO cells (Fig. 5a). This increase in p21^{Cip1} protein could be accounted for by a concomitant increase in its levels of messenger RNA (Fig. 5b). Consistent with these findings, Cdk2-associated activities were markedly reduced and Rb was found to be predominantly in its hypophosphorylated state (Fig. 5a, c). Furthermore, cyclin-B-associated kinase activity was also significantly reduced in TKO cells, even though a large

population of the cells possessed either an S phase or G2 content of DNA. These results might, at least in part, explain the apparent growth arrest that occurs through various phases of the cell cycle, namely in G1, S and G2/M of TKO cells. The fact that overexpression of cyclin E/Cdk2 could drive TKO cells into S phase (Fig. 5d) suggests that the upregulation of p21^{Cip1} protein is probably a relevant consequence resulting from the ablation of E2F1, E2F2 and E2F3.

The status of Rb-E2F-associated DNA binding activities were also assessed in these cells. Consistent with previous studies, electrophoretic mobility shift assays (EMSA) of lysates from control- or Cre-treated *E2F1^{-/-}E2F2^{-/-}E2F3^{fl/fl}* cells synchronized by serum deprivation, revealed the characteristic Rb-related p130-E2F4/5 protein complexes¹⁴. These G0-specific complexes are thought to recruit histone deacetylase and remodelling activities, and are presumed to mediate transcriptional repression of E2F target genes¹⁹⁻²⁵. In contrast to control-treated MEFs, serum stimulation of TKO cells did not lead to the dissociation and disappearance of p130-E2F4/5 complexes nor to the appearance of the S-phase-specific p107-E2F4 complex (Fig. 5e). These findings are consistent with the observed increase in p21^{Cip1} protein and decrease in Cdk activity and Rb phosphorylation (Fig. 5a, c). We propose that E2F activators mediate cell cycle progression by two mechanisms: first, they can directly activate cell-cycle-dependent gene expression, and second, they can activate a positive feedback loop, through inhibition of p21^{Cip1} protein accumulation, that would promote Rb phosphorylation and complete derepression of Rb-E2F target genes. The decrease in E2F target gene expression observed in TKO cells (Fig. 3a) could be viewed to result from both the continued Rb-mediated transcriptional repression and the absence of E2F-mediated transcription activation. Although our results establish the critical nature of E2F1, E2F2 and E2F3 in the control

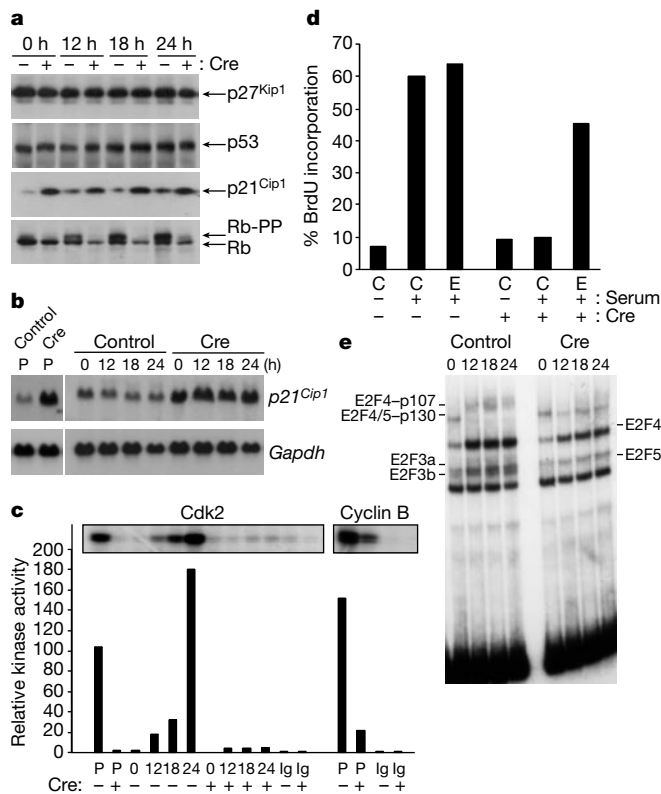


Figure 5 Loss of E2Fs leads to an elevation of p21^{Cip1}. **a**, Western blots of control- or Cre-retrovirus-infected *E2F1*^{-/-}*E2F2*^{-/-}*E2F3*^{+/+} MEFs using antibodies against the indicated cell cycle regulators. Rb-PP, phosphorylated form of Rb. **b**, p21 Northern blot of *E2F1*^{-/-}*E2F2*^{-/-}*E2F3*^{+/+} MEFs that were treated as in **a**. P, proliferating conditions. **c**, Kinase assays of *E2F1*^{-/-}*E2F2*^{-/-}*E2F3*^{+/+} MEFs treated as in **a**. Ig, rabbit immunoglobulin-γ as controls. The graph represents the relative kinase activity. **d**, BrdU incorporation assays of *E2F1*^{-/-}*E2F2*^{-/-}*E2F3*^{+/+} MEFs that were infected with a control (-) or a Cre retrovirus (+). Serum-starved cells were infected with adenoviruses expressing cyclin E and Cdk2 (E) or with a control adenovirus (C). Adenovirus-infected cells were incubated with BrdU in either 0.2% serum (-) or 15% serum (+) for 24 h, and processed for immunohistochemistry. **e**, *E2F1*^{-/-}*E2F2*^{-/-}*E2F3*^{+/+} MEFs were treated as in **a**, and were assayed for E2F DNA-binding activity by EMSA using an E2F-specific ³²P-labelled DNA probe.

of cellular proliferation, the relative importance of E2F-mediated transcriptional repression versus activation remains to be determined. The mechanism by which E2F family members regulate p21^{Cip1} expression and its *in vivo* consequences will be an important topic of future experimentation.

Although a role for E2F in the regulation of the cell cycle and proliferation has been speculated for over a decade^{1,2,26–28}, the complexity of the E2F network has precluded previous loss-of-function mouse models from demonstrating the essentiality for individual E2F family members in mammalian cell proliferation. The ‘conditional’ gene knockout strategy described here allowed us to circumvent detrimental consequences that arise from the inactivation of multiple E2F family members in mice. By making genetic modifications to the entire E2F activator subclass, as opposed to individual members, we provide direct genetic evidence suggesting that E2F activators are essential for cell cycle progression, proliferation and development. □

Methods

Construction of the targeting vector

We used a triple *loxP* vector system (R. Premont, personal communication) to construct our targeting vector. We used a 1.7-kilobase (kb) *EcoRV*–*SpeI* fragment as the short recombination arm, a 2.3-kb *SpeI* fragment, which includes exon 3, as the floxed fragment,

and a 6-kb *SpeI* fragment spanning exons 4 and 5 as the long recombination arm. The final targeting vector shown in Fig. 1a was constructed using standard subcloning procedures. We verified all of the constructs by restriction analysis and sequencing.

Generation of E2F3 knockout mice

Strain 129 E14 embryonic stem (ES) cells were electroporated with 50 μg *NotI* linearized targeting vector. Homologous recombination was selected with G418 and diphtheria toxin and verified by Southern blot and PCR analysis. The properly integrated ES cell clones were transiently transfected with a Cre-expressing plasmid. After negative selection with gancyclovir, clones with either a conventional null allele or a conditional null allele were screened and confirmed by Southern blot and PCR analysis. Appropriate ES cell clones were injected into E3.5 C57BL/6 blastocysts that were subsequently implanted into foster mothers. We bred the resulting chimaeras with C57BL/6 females to achieve germline transmission. Genotypic analysis of offspring was performed by Southern analysis and multiplex PCR using the three primers shown in Fig. 1a (primer A, 5′-GTGGCTGG AAGGGTGC CAAG-3′; primer B, 5′-TGAATCATGGACAGAGCCAGG-3′; and primer C, 5′-GATTGATTCTGGGTTGTCAGG-3′).

MEF generation and establishment of MEF cell lines

Primary MEFs were isolated from E13.5 embryos using standard methods. The relative contributions from 129/Sv and C57BL/6 genetic backgrounds in each of the E2F-deficient MEF lines used in this study are very similar. Moreover, the experiments presented here were repeated in at least two different MEF preparations, most of which were from different litters. We generated immortalized cell lines from primary MEFs using the 3T9 cell line preparation protocol.

Retroviral infections

Full-length complementary DNAs for Cre recombinase, Myc-tagged versions of mouse E2F3a and E2F3b and HA-tagged versions of human E2F1, E2F2 and E2F3a were subcloned into the pBabe retroviral vector containing either a puromycin-(pBpuro), hygromycin-(pBhygro), or phleomycin-resistant gene (pBbleo). High-titre viruses were produced by transient transfection of retroviral constructs into the Phoenix-Eco packaging cell line as described previously²⁹. We infected MEFs with the retrovirus using standard methods. Infected cells were then selected for a total of five days in the presence of one or more antibiotics using the following concentrations: 2.5 μg ml⁻¹ for puromycin, 400 μg ml⁻¹ for hygromycin and 25 μg ml⁻¹ for phleomycin.

Proliferation assays

Immortalized MEFs were seeded at 7 × 10⁴ cells per 60-mm dish. Duplicate plates of cells were counted daily and were replated every 72 h at the same density of the initial plating. Colony formation assays were performed by plating 600 or 3,000 immortalized cells per 100-mm dish with five dishes at each concentration. Cells were cultured in DMEM with 15% fetal bovine serum (FBS) until colonies formed, and then stained with 5 mg ml⁻¹ crystal violet in 20% methanol. The number of colonies arising in five plates was determined and the mean and standard deviations of five cultures from one representative experiment are reported. Single colonies were isolated from parallel, 96-well culture plates. DNA was collected from individual colonies and was genotyped by PCR.

Serum starvation and serum stimulation

Subconfluent MEFs were synchronized by incubation in DMEM with 0.2% FBS for either 60 h (for primary MEFs) or 72 h (for immortalized MEFs). Synchronized cells were then stimulated to proliferate by the addition of DMEM supplemented with 15% FBS. Cells were collected at different time points after serum stimulation and were processed for BrdU incorporation assays¹⁴, flow cytometry¹⁴, histone H1 kinase assays¹⁴, EMSA³⁰, western blots, or northern blots. For BrdU incorporation assays, we counted at least 300 4,6-diamidino-2-phenylindole (DAPI) counter-stained nuclei for each time point.

Western and northern blot analyses

Cell protein lysates were separated in SDS acrylamide gels and blotted into polyvinylidene fluoride membranes. Blots were incubated in blotto buffer (5% skim milk in Tris-buffered saline) with antibodies specific for E2F3 (SC-878, Santa Cruz), phospho-Akt (Cell Signalling, no. 9271L), phospho-Erk (Cell Signalling, no. 9101S), p21^{Cip1} (M-19 and C-19, Santa Cruz), p27^{Kip1} (Transduction Laboratory), p53 (14461C, PharMingen and Ab-1, Oncogene), Rb (G3-245, PharMingen), c-Myc-epitope (C-33, Santa Cruz), HA epitope (Y-11, Santa Cruz), cyclin B1 (GNS1, Santa Cruz) and Cdk2 (M2, Santa Cruz). The primary antibodies were then detected using horseradish-peroxidase-conjugated secondary antibodies and ECL reagent as described by the manufacturer (Amersham).

Total RNA for northern blot analysis was isolated using TRIzol (GibcoBRL), and mRNA was subsequently purified using the PolyAtract mRNA isolation system as described by the manufacturer (Promega). Purified mRNA was separated on a 1% agarose gel containing 6% formaldehyde and transferred onto a GeneScreen membrane (NEN Life Science Products). The cDNA probes were labelled using Prime-It RmT (Stratagene) with 50 μCi [α-³²P]dCTP.

Statistical analysis

We performed statistical analyses using Splus 4.5 (Mathsoft). Observed versus expected progeny proportions were tested as deviations from the null binomial distributions conditioned on the fixed number of examined progeny. Confidence intervals were based on standard normal approximations. Cell growth (control versus Cre) kinetics for each

genotype group were compared as follows: the ratios of cell numbers at each time point and the previous time point were compared in control versus Cre to account for serial correlation. Graphical summaries revealed that the ratios for control versus Cre were positively correlated, and we used two-sided *t*-comparisons (9 degrees of freedom) to compare the ratios. The average control versus Cre growth rates showed a monotonically increasing trend across the genotypes shown. We applied a simple nonparametric test bed on all possible orderings. Similar techniques were applied for per cent BrdU incorporation after serum stimulation, using the differences of successive observations to account for serial correlation. Percentages were converted to the logarithmic scale and time points after the apparent detection threshold at 8 h were used.

Received 30 July; accepted 25 September 2001.

- Dyson, N. The regulation of E2F by pRB-family proteins. *Genes Dev.* **12**, 2245–2262 (1998).
- Nevins, J. R. Toward an understanding of the functional complexity of the E2F and retinoblastoma families. *Cell Growth Differ.* **9**, 585–593 (1998).
- DeGregori, J., Leone, G., Miron, A., Jakoi, L. & Nevins, J. R. Distinct roles for E2F proteins in cell growth control and apoptosis. *Proc. Natl Acad. Sci. USA* **94**, 7245–7250 (1997).
- Duronio, R. J., O'Farrell, P. H., Xie, J. E., Brook, A. & Dyson, N. The transcription factor E2F is required for S phase during *Drosophila* embryogenesis. *Genes Dev.* **9**, 1445–1455 (1995).
- Royzman, I., Whittaker, A. J. & Orr-Weaver, T. L. Mutations in *Drosophila* DP and E2F distinguish G1–S progression from an associated transcriptional program. *Genes Dev.* **11**, 1999–2011 (1997).
- Field, S. J. *et al.* E2F-1 functions in mice to promote apoptosis and suppress proliferation. *Cell* **85**, 549–561 (1996).
- Humbert, P. O. *et al.* E2F4 is essential for normal erythrocyte maturation and neonatal viability. *Mol. Cell* **6**, 281–291 (2000).
- Humbert, P. O. *et al.* E2F3 is critical for normal cellular proliferation. *Genes Dev.* **14**, 690–703 (2000).
- Leone, G. *et al.* Myc requires distinct E2F activities to induce S phase and apoptosis. *Mol. Cell* **8**, 105–113 (2001).
- Lindeman, G. J. *et al.* A specific, nonproliferative role for E2F-5 in choroid plexus function revealed by gene targeting. *Genes Dev.* **12**, 1092–1098 (1998).
- Rempel, R. E. *et al.* Loss of E2F4 activity leads to abnormal development of multiple cellular lineages. *Mol. Cell* **6**, 293–306 (2000).
- Yamasaki, L. *et al.* Tumor induction and tissue atrophy in mice lacking E2F-1. *Cell* **85**, 537–548 (1996).
- Lees, J. A. *et al.* The retinoblastoma protein binds to a family of E2F transcription factors. *Mol. Cell Biol.* **13**, 7813–7825 (1993).
- Leone, G. *et al.* E2F3 activity is regulated during the cell cycle and is required for the induction of S phase. *Genes Dev.* **12**, 2120–2130 (1998).
- Leone, G. *et al.* Identification of a novel E2F3 product suggests a mechanism for determining specificity of repression by Rb proteins. *Mol. Cell Biol.* **20**, 3626–3632 (2000).
- Lukas, C. *et al.* Accumulation of cyclin B1 requires E2F and cyclin-A-dependent rearrangement of the anaphase-promoting complex. *Nature* **401**, 815–881 (1999).
- Ishida, S. *et al.* Role for E2F in control of both DNA replication and mitotic functions as revealed from DNA microarray analysis. *Mol. Cell Biol.* **21**, 4684–4699 (2001).
- Muller, H. *et al.* E2Fs regulate the expression of genes involved in differentiation, development, proliferation, and apoptosis. *Genes Dev.* **15**, 267–285 (2001).
- Brehm, A. *et al.* Retinoblastoma protein recruits histone deacetylase to repress transcription. *Nature* **391**, 597–601 (1998).
- Harbour, J. W. & Dean, D. C. Chromatin remodeling and Rb activity. *Curr. Opin. Cell Biol.* **12**, 685–689 (2000).
- Luo, R. X., Postigo, A. A. & Dean, D. C. Rb interacts with histone deacetylase to repress transcription. *Cell* **92**, 463–473 (1998).
- Magnaghi-Jaulin, L. *et al.* Retinoblastoma protein represses transcription by recruiting a histone deacetylase. *Nature* **391**, 601–605 (1998).
- Weintraub, S. J., Prater, C. A. & Dean, D. C. Retinoblastoma protein switches the E2F site from positive to negative element. *Nature* **358**, 259–261 (1992).
- Weintraub, S. J. *et al.* Mechanism of active transcriptional repression by the retinoblastoma protein. *Nature* **375**, 812–815 (1995).
- Zhang, H. S., Postigo, A. A. & Dean, D. C. Active transcriptional repression by the Rb–E2F complex mediates G1 arrest triggered by p16INK4a, TGF β , and contact inhibition. *Cell* **97**, 53–61 (1999).
- Tsai, K. Y. *et al.* Mutation of E2F-1 suppresses apoptosis and inappropriate S phase entry and extends survival of Rb-deficient mouse embryos. *Mol. Cell* **2**, 293–304 (1998).
- Yamasaki, L. *et al.* Loss of E2F-1 reduces tumorigenesis and extends the lifespan of Rb1(+/-) mice. *Nature Genet.* **18**, 360–364 (1998).
- Ziebold, U., Reza, T., Caron, A. & Lees, J. A. E2F3 contributes both the inappropriate proliferation and to the apoptosis arising in Rb mutant embryos. *Genes Dev.* **15**, 386–391 (2001).
- Pear, W. S., Nolan, G. P., Scott, M. L. & Baltimore, D. Production of high-titer helper-free retroviruses by transient transfection. *Proc. Natl Acad. Sci. USA* **90**, 8392–8396 (1993).
- Nevins, J. R., DeGregori, J., Jakoi, L. & Leone, G. in *Methods in Enzymology* (ed. Dunphy, W. G.) 678 (Academic, San Diego, 1997).

Supplementary Information accompanies the paper on Nature's website (<http://www.nature.com>).

Acknowledgements

We are grateful to R. Premont for providing the *loxP* vectors. We thank C. Bock for assistance in generating the *E2F3* chimeric mice; C. Brown and L. Jakoi for various technical assistance; and M. Weinstein for critical comments on the manuscript. This work was supported by grants from the National Institutes of Health (NIH) (G.L.). L.W. was supported by an NIH award, C.T. was supported by the Up on the Roof Human Cancer Genetics Postdoctoral Fellowship, J.R.N. is an investigator of the Howard Hughes Medical Institute, and G.L. is a V-Foundation and Pew Charitable Trust Scholar.

Correspondence and requests for materials should be addressed to G.L. (e-mail: Leone-1@medctr.osu.edu).

A phosphate transporter expressed in arbuscule-containing cells in potato

Christine Rausch*†, Pierre Daram*†, Silvia Brunner†, Jan Jansa†, Maryse Laloi‡, Georg Leggewie§, Nikolaus Amrhein|| & Marcel Bucher†

† Federal Institute of Technology (ETH) Zurich, Institute of Plant Sciences, Experimental Station Eschikon 33, 8315 Lindau, Switzerland
 § Max Planck Institute of Plant Molecular Physiology, 14424 Potsdam, Germany
 || Federal Institute of Technology (ETH) Zurich, Institute of Plant Sciences, Universitätsstrasse 2, 8092 Zurich, Switzerland
 * These authors contributed equally to the work
 ‡ Present address: Nestlé Research Center, Lausanne, PO Box 44, Vers-chez-les-Blanc, 1000 Lausanne 26, Switzerland

Arbuscular mycorrhizas are the most common non-pathogenic symbioses in the roots of plants. It is generally assumed that this symbiosis facilitated the colonization of land by plants¹. In arbuscular mycorrhizas, fungal hyphae often extend between the root cells and tuft-like branched structures (arbuscules) form within the cell lumina that act as the functional interface for nutrient exchange. In the mutualistic arbuscular-mycorrhizal symbiosis the host plant derives mainly phosphorus from the fungus, which in turn benefits from plant-based glucose². The molecular basis of the establishment and functioning of the arbuscular-mycorrhizal symbiosis is largely not understood. Here we identify the phosphate transporter gene *StPT3* in potato (*Solanum tuberosum*). Functionality of the encoded protein was confirmed by yeast complementation. RNA localization and reporter gene expression indicated expression of *StPT3* in root sectors where mycorrhizal structures are formed. A sequence motif in the *StPT3* promoter is similar to transposon-like elements, suggesting that the mutualistic symbiosis evolved by genetic rearrangements in the *StPT3* promoter.

Phosphorus is usually taken up in the form of orthophosphate (Pi). It is well known that Pi transport into the root is mediated by a secondary transport mechanism dependent on the activity of the

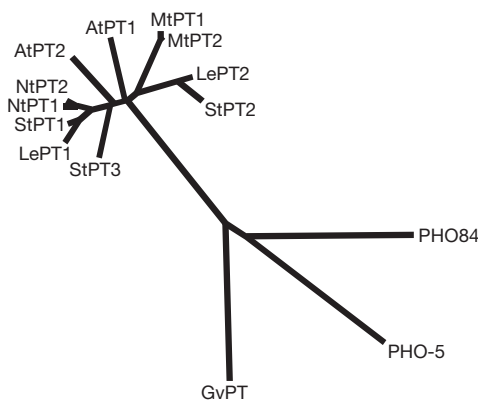


Figure 1 Phylogenetic relationship of *StPT3* with other Pi transporters. Phylogenetic analysis of plant Pht1 and related high-affinity Pi transporters from fungal species. Protein names are followed by SwissProt (SP) or GenBank (GB) accession numbers: LePT1 (O24029, SP) and LePT2 (O22549, SP) from *Lycopersicon esculentum*; NtPT1 (AAF74025, GB) and NtPT2 (BAA86070, GB) from *Nicotiana tabacum*; StPT1 (Q43650, SP), StPT2 (Q41479, SP) and StPT3 (AJ318822, GB) from *Solanum tuberosum*; MtPT1 (O22301, SP) and MtPT2 (O22302, SP) from *Medicago truncatula*; AtPT1 (Q96302, SP) and AtPT2 (Q96303, SP) from *Arabidopsis thaliana*; PHO84 (P25297, SP) from *Saccharomyces cerevisiae*; PHO-5 (L36127, GB) from *Neurospora crassa*, and GvPT (U38650, GB) from *Glomus versiforme*.